Identification of Phosphorus Sources in a Watershed Using a Phosphate Oxygen Isoscape Approach

Takuya Ishida,*,[†] Yoshitoshi Uehara,[†] Tomoya Iwata,[‡] Abigail P. Cid-Andres,[§] Satoshi Asano,[∥]
Tohru Ikeya,[†] Ken'ichi Osaka,[⊥] Jun'ichiro Ide,[#] Osbert Leo A. Privaldos,[▽] Irisse Bianca B. De Jesus,[○]
Elfritzson M. Peralta,[○] Ellis Mika C. Triño,[○] Chia-Ying Ko,[◆] Adina Paytan,[¶] Ichiro Tayasu,[†]
and Noboru Okuda[†]

[†]Research Institute for Humanity and Nature, 457-4, Motoyama, Kamigamo, Kyoto, 603-8047, Japan

[‡]Faculty of Life and Environmental Science, University of Yamanashi, 4-4-37, Takeda, Kofu, Yamanashi 400-8510, Japan

[§]Department of Physical Sciences, College of Science, Polytechnic University of the Philippines, Anonas Street. Sta. Mesa, Manila 1016, Philippines

[∥]Lake Biwa Environment Research Institute, 5-34, Yanagasaki, Ohtsu, Shiga 520-0022, Japan

[⊥]School of Environmental Sciences, The University of Shiga Prefecture, 2500, Hasaka, Hikone, Shiga 522-8533, Japan

[#]Institute of Decision Science for a Sustainable Society, Kyushu University, 394, Tsubakuro, Sasaguri, Fukuoka 811-2415, Japan

[▽]Laguna Lake Development Authority, National Ecology Center, East Avenue, Diliman, Quezon City, 1101, Philippines

[○]The Graduate School, University of Santo Tomas, España Boulevard, Manila 1015, Philippines

[◆]Institute of Fisheries Science & Department of Life Science, National Taiwan University, No. 1, Sec. 4, Roosevelt Road, Taipei 10617, Taiwan

[¶]Institute of Marine Sciences, University of California Santa Cruz, 1156 High Street, Santa Cruz, California 95064, United States

S *Supporting Information*

ABSTRACT: Identifying nonpoint phosphorus (P) sources in a watershed is essential for addressing cultural eutrophication and for proposing best-management solutions. The oxygen isotope ratio of phosphate ($\delta^{18}O_{PO_4}$) can shed light on P sources and P cycling in ecosystems. This is the first assessment of the $\delta^{18}O_{PO_4}$ distribution in a whole catchment, namely, the Yasu River Watershed in Japan. The observed $\delta^{18}O_{PO_4}$ values in the river water varied spatially from 10.3‰ to 17.6‰. To identify P sources in the watershed, we used an isoscape approach involving a multiple-linear-regression model based on land use and lithological types. We constructed two isoscape models, one using data only from the whole watershed and the other using data from the small tributaries. The model results explain 69% and 96% of the spatial variation in the river water $\delta^{18}O_{PO_4}$. The lower R^2 value for the whole watershed model is attributed to the relatively large travel time for P in the main stream of the lower catchment that can result in cumulative biological P recycling. Isoscape maps and a correlation analysis reveal the relative importance of P loading from paddy fields and bedrock. This work demonstrates the utility of $\delta^{18}O_{PO_4}$ isoscape models for assessing nonpoint P sources in watershed ecosystems.
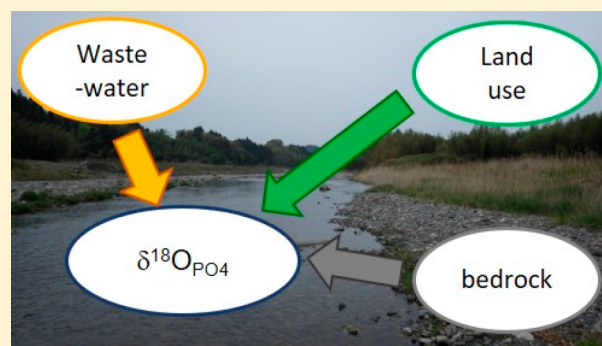
1.0. INTRODUCTION

Anthropogenic phosphorus (P) loads have increased in many watersheds because of industrialization and urbanization, resulting in serious cultural eutrophication issues in aquatic ecosystems. To mitigate such cultural eutrophication, watershed management has been practiced to reduce P loads from point sources through institutional and technological approaches, including (i) laws to regulate nutrient loadings and (ii) installing wastewater treatment plants (WWTPs).[1−3]

Nevertheless, compared to point sources, it has been more difficult to regulate nonpoint P sources (e.g., anthropogenic loads from agricultural and urban activities, natural loads from forests and bedrock, and atmospheric deposition[4]) primarily
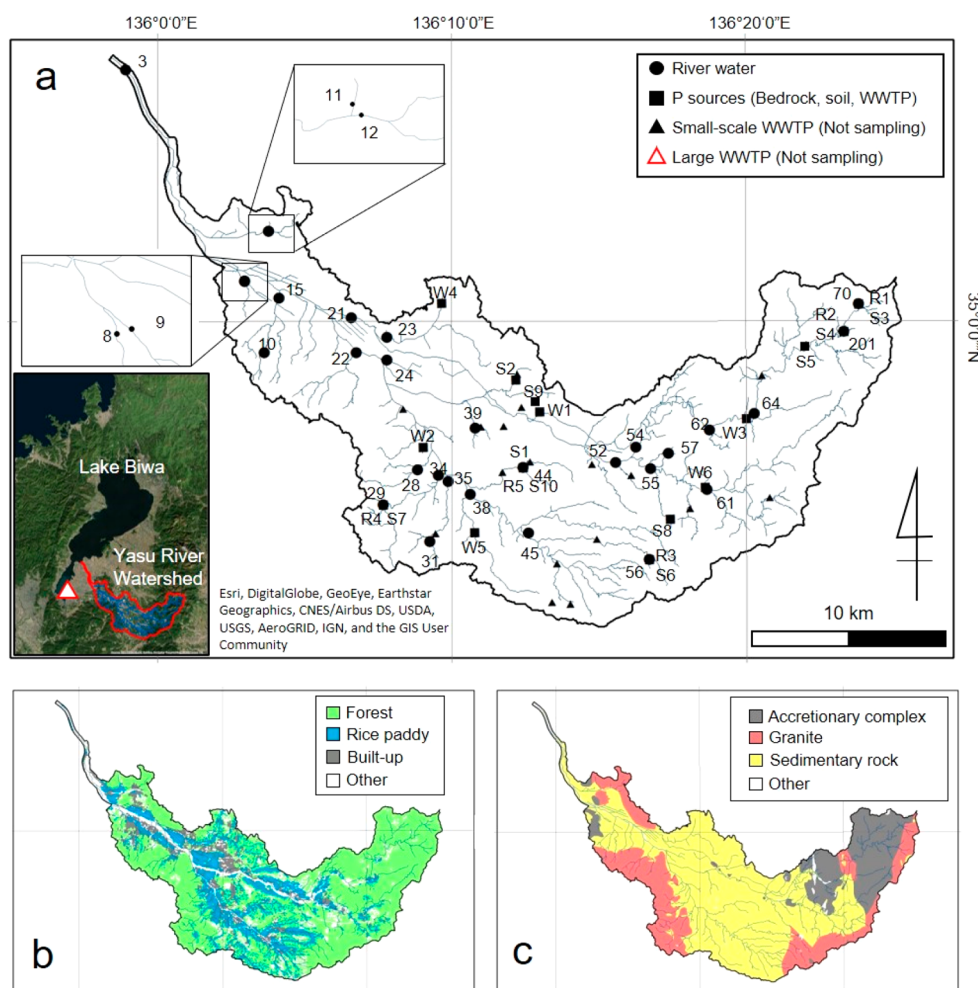
Figure 1. (a) Map of sampling sites for river water (circles) and potential P sources (squares) and locations of large (open red triangle in small window representing Lake Biwa) and small-scale (closed triangles) wastewater treatment plants (WWTPs) in the catchment of the Yasu River tributary to Lake Biwa in Shiga, Japan. (b) GIS map of land use. (c) GIS map of geological properties. See Table S1 for site IDs and GIS data, and see Tables S2−S4 for abbreviations of sample types.

because it is difficult to assess the contribution of each nonpoint source to the total load. Therefore, to overcome this limitation related to P pollution, apportioning point and nonpoint sources and long-term assessment of these contributions are important.[3,5,6]

Studies are increasingly using the oxygen isotope ratio of phosphate ($\delta^{18}O_{PO_4}$) to understand P dynamics in both aquatic and terrestrial ecosystems (refs 7−10 and reference therein). Because the P−O bonds in phosphate do not easily hydrolyze at earth's typical surface temperatures and pressures, $\delta^{18}O_{PO_4}$ values in environmental samples are imprinted with the isotopic signatures of the P sources provided P uptake and utilization by organisms is limited.[7,9] Biological processes mediated by enzymes that cleave the P−O bonds cause large isotopic fractionation.[11−15] For example, intracellular activity of inorganic pyrophosphatase (PPase) can alter the isotopic signatures of environmental phosphate samples and appears to dominate the $\delta^{18}O_{PO_4}$ signature of inorganic phosphate (Pi) pool in most natural aquatic systems.[7,16] The $\delta^{18}O_{PO_4}$ of the Pi pool that has been catalyzed by PPase reaches temperature-dependent isotope equilibrium on relatively short time scales, and several equations have been proposed to estimate the equilibrium value.[14,15] Those equations can be used to

estimate the biological recycling of P in ecosystems based on the extent to which source isotope signatures are overwritten by such biological processes and are approaching the equilibrium value.[7]

$\delta^{18}O_{PO_4}$ has not been used much in freshwater systems, such as rivers and lakes, primarily because of inorganic and/or organic compounds in these freshwater samples that interfere with the precipitation of phosphate as pure silver phosphate used for isotope analysis.[9] This problem can be overcome partially by adding more purification steps;[9] however, using the $\delta^{18}O_{PO_4}$ system remains challenging for systems with low dissolved Pi concentration and high concentration of dissolved organic matter.[17,18] Despite these difficulties, P sources can be identified using $\delta^{18}O_{PO_4}$ in subcatchments with measurable P loads.[6,17−21] To identify nonpoint P sources from natural and anthropogenic loading in a watershed, it is important to determine the sources of P from head catchments that can be sensitive to human disturbance because of their small water volume[22] to the downstream catchments that are typically influenced by multiple P sources.

In the present study, we conducted synoptic sampling of river water and potential P sources in the whole catchment of the Yasu River, a tributary of Lake Biwa in Japan (Figure 1a) to

identify natural and anthropogenic P sources, especially nonpoint sources, using $\delta^{18}O_{PO_4}$. Although isotope mixing models have been used previously to quantify the relative contribution of P sources in simple and small-scale systems with only a few P sources,[21,23] this approach has yet to yield realistic solutions in complex watershed systems. Here, we use a $\delta^{18}O_{PO_4}$ isoscape (isotopic landscape) approach to assess P sources throughout the entire catchment of the Yasu River. The isoscape approach allows us to visualize the contribution of sources and biogeochemical processes and to link the spatial pattern of river water $\delta^{18}O_{PO_4}$ values to site characteristics such as land use and lithological type.[24−26]

2.0. MATERIALS AND METHODS

2.1. Study Site. Our study area encompasses the entire catchment of the Yasu River, the largest tributary in Lake Biwa Watershed (LBW) in Japan (Figure 1a). Lake Biwa was oligotrophic until the 1950s, but since then, cultural eutrophication due to rapid industrialization and urbanization has been prevalent.[5] In 1979, Shiga Prefecture (governing this watershed) imposed legislation to mitigate this cultural eutrophication. It then promoted the installation of wastewater treatment plants (WWTPs) to reduce nutrient loadings from industrial and domestic point sources. From the 1980s to the present, the total P load into the lake has been halved.[27]

The Yasu River originates from Mt. Gozaisyo, at 1213 m elevation. Its river length and catchment area are 65.3 km and 387 km^2, respectively. Precipitation and temperature range from 1618 mm and 15.5 °C in the lower (Ohtsu) catchment to 1637 mm and 13.6 °C in the upper (Tsuchiyama) catchment (annual means from 2007 to 2016). The catchment is covered by forest (55%), cropland (24%), and built-up (11%) land uses (Figure 1b). The dominant crop in the catchment is rice, occupying 91% of the cropland area. The irrigation period of rice paddies is typically from April to September. The Yasu River Watershed (YRW) is characterized by three lithological types: an accretionary complex (18%), granite (22%), and sedimentary rocks (59%) (Figure 1c).

Domestic wastewater in this catchment is treated at one large WWTP as well as in many smaller-scale WWTPs. The large WWTP, located outside the catchment (Figure 1a), services 91.4% of the human population in five local government areas overlapping YRW, and its effluent is discharged into the nearby lake basin not impacting the Yasu River.[27] The smaller WWTPs are located in the rural areas of the upper catchment (Figure 1a), and their effluents are discharged directly into the nearby stream tributaries of the Yasu River.

2.2. Sample Collection. River water samples for $\delta^{18}O_{PO_4}$ analysis were collected using a plastic bucket and then emptied into 20 L polyethylene containers at 30 sites representing first- to fifth-order streams whose catchments differ in land use and lithological type (Figure 1). The sampling sites were established upstream of river confluences to uniquely characterize respective tributaries to the main stem. A synoptic survey was conducted in May 2016 at the beginning of the paddy irrigation period. The sample volumes were 20−40 L depending on the soluble reactive phosphate (SRP) concentration at each site, measured prior to sample collection. River water samples were collected from shallow channel units (e.g.,

riffle, rapid, or glide) in each sampling site where river waters are well mixed by turbulent flow.

Locations of the water sampling sites were selected to represent potential nonpoint source end members in the watershed based on a specific land use, lithological distribution, and P loads according to a report of Shiga Prefecture estimating the P loads into LBW using a simulation model.[28] Potential sources that contribute dissolved Pi to the river/ tributaries in the catchment, composed of bedrock, forest-floor soils, paddy soils, fertilizers, and WWTP effluents, were also collected (Figure 1a and Tables S1−S4). In head catchments characterized by a single rock type [sites 29 and 56 (IDs: R4 and R3) for granite and sites 70 and 201 (R1 and R2) for accretionary complex rocks], a riverbed gravel was collected as a representative of the lithology. This gravel is assumed to be a better representative of the rocks in the subcatchment than the bedrock because this sample integrates and encompasses the bedrock heterogeneity, if any exists. To remove organic matter attached to the riverbed gravel, the samples were sieved into 1−4.75 mm fraction and then rinsed thoroughly with ultrapure water (UPW). To represent the sedimentary rocks in the basin, a sample (R5) was handpicked from a fault area in the sedimentary rock layer near site 44 (Figure 1) because other rock exposures were not attainable. Forest soil samples were collected in the areas covered by the Japanese cedar forests to represent sites with different bedrock types, thus possibly affecting the $\delta^{18}O_{PO_4}$ value in soils.[29] The soil samples were collected from the A horizon (about 0−10 cm depth) at three points per site (S3−S10; Figure 1) and then combined as one sample. The samples of rice paddy soil were collected from the depth of about 10 cm corresponding to the upper root layer at the center of two different paddy fields (S1 and S2) in December 2015, which is a nonirrigation period to avoid crop damage. These rice paddies are owned by different famers, allowing us to examine differences in their farming practices on $\delta^{18}O_{PO_4}$ value. The farmers also provided us with manufactured organic (F1) and chemical (F2) fertilizers commonly used in Shiga Prefecture. These organic and chemical fertilizers contain 8% and 28% P, respectively, as indicated by the manufacturer. The water-soluble Pi content of these fertilizers analyzed in this study is presented in Table S4. We also obtained a stock solution (F3) of the manufactured chemical fertilizers from the company that supplies around 90% of the products distributed by the Japan Agricultural Cooperatives (JA) in Shiga Prefecture (JA, personal communication). WWTP effluent samples (5 L each) were collected with a plastic bucket directly from a final storage pool at six (W1−W6) of the small-scale WWTPs in the rural areas of the upper catchment (Figure 1a) in August 2018 and kept in 10 L polyethylene containers until analysis.

To calculate the theoretical expected isotope equilibrium values of $\delta^{18}O_{PO_4}$ of different samples, river water, WWTP effluent, and paddy irrigation water samples were collected for water oxygen isotope ratios ($\delta^{18}O_{H_2O}$). The water temperature in the river was measured using a logger (UA-002-64; Hobo) installed at each of the 30 sampling sites for more than 3 days to obtain the daily average. For the WWTP effluent samples, the water temperature was measured using a multiprobe (ProDSS; YSI Inc., Unite States). The temperature of the irrigation water was measured with the logger set at the three rice paddies in the catchment of site 44 during the irrigation period.

2.3. Sample Preparation. Water samples were filtered through 0.2 μm membrane filters (Advantec) for measurement of $\delta^{18}O_{H_2O}$ and SRP concentration and through 0.45 μm membrane filters (Advantec) for $\delta^{18}O_{PO_4}$ analysis, within 24 h from collection. Following the filtration, $MgCl_2$ was added to the samples used for $\delta^{18}O_{PO_4}$ analysis, and the pH increased to ~10.5 to remove the phosphate as brucite (magnesium-induced coprecipitation, MAGIC).[30]

The rock and gravel samples were washed using UPW, dried at 50 °C, and ground to powder using a multibead shocker (Yasui Kikai, Japan) with tungsten carbide beads to homogenize the samples and to enhance the reaction between extraction solution and the sample. The samples were stored at room temperature until analysis. The powdered samples were immersed in 1 M HCl for 16 h to extract the soluble Pi.[31] Soil samples were air-dried and sieved through a 2 mm mesh and stored at room temperature until analysis (~1 year). Labile and weakly absorbed Pi in the soils was extracted with a 0.5 M $NaHCO_3$ solution.[31] The $NaHCO_3$ extractable Pi in our study may include microbial Pi, because soil drying lyses bacterial cells.[32] Although storing soil at room temperature without drying processes changes the $\delta^{18}O_{PO_4}$ value of labile Pi (~3.6‰),[33] the changes in the $\delta^{18}O_{PO_4}$ values of $NaHCO_3$ extractable Pi in our soil samples during storage should have been limited because of completely drying the samples. The organic and chemical fertilizers were dried at 50 °C and powdered to extract their labile phosphate with the UPW.

2.4. Sample Analysis. The SRP concentration of each sample was measured using the molybdenum-blue method[34] on a microplate spectrophotometer (Multiskan GO; Thermo Fisher Scientific). The detection limit of this devise is 0.08 μmol L^{-1}, and the repeatability based on duplicate analyses of the same samples (±SD) is ±0.02 μmol L^{-1}. For the $\delta^{18}O_{PO_4}$ analysis, inorganic phosphate samples were converted to Ag_3PO_4 according to McLaughlin et al.[30] with the addition of a solid-phase extraction step to remove dissolved organic matter (Figure S1).[35]

The $\delta^{18}O_{PO_4}$ values reported relative to the Vienna standard mean ocean water (VSMOW) of the Ag_3PO_4 samples were measured using a TC/EA-IRMS (thermal conversion elemental analyzer connected to a Delta plus XP via ConFlo III, Thermo Fisher Scientific) at the Research Institute for Humanity and Nature (RIHN). Three internal standards with values of 8.3 ± 0.29‰, 14.4 ± 0.14‰, and 23.1 ± 0.27‰ were used for calibration and normalization after calibration with two independently calibrated standards (STDL: 11.3 ± 0.15‰; STDH: 20.0 ± 0.25‰) reported by McLaughlin et al.[30] The analytical precision (±SD) was ±0.4‰. Three replicates of rock and soil samples were prepared for $\delta^{18}O_{PO_4}$ analysis. The standard deviation of the triplicate measurements was less than 0.5‰, demonstrating the reliability and reproducibility of the method.

$\delta^{18}O_{H_2O}$ values were measured using a water isotope analyzer (L2120-I; Picarro, United States) with an analytical precision of 0.05‰. The expected equilibrium values ($\delta^{18}O_{PO_4Eq}$) were estimated using the following empirical equation:[14]

$$\delta^{18}O_{PO_4Eq} = \delta^{18}O_{H_2O} - (T + 273.15)/4.3 + 25.9 \quad (1)$$

where $\delta^{18}O_{H_2O}$ is the oxygen isotope ratio (‰) of ambient water and T (K) is the water temperature.

2.5. Isoscape Approach. Land cover and lithological type in the watershed were determined for each sampling site using a geographic information system (ArcGIS 10.2; ESRI Japan). We used a 1/50 000 digitized vegetation map obtained from the Biodiversity Center of Japan to determine the areal proportion of four land-cover types (forest, paddy field, built-up, other) for the catchment of each sampling site. We also used a 1/200 000 digital geological map published by the Geological Survey of Japan to calculate the proportional area of each lithological type (accretionary complex, granite, sedimentary rock) for each catchment.

To delineate the $\delta^{18}O_{PO_4}$ isoscapes of the entire river system, we used a multiple regression analysis incorporating as explanatory variables the proportional areas of the land cover (forest, paddy field, and built-up) and lithological types (accretionary complex, granite, and sedimentary rock) that are deemed to be potential nonpoint P sources in the YRW. We constructed two models, (i) a watershed model and (ii) a tributary model, based on the $\delta^{18}O_{PO_4}$ values of (i) all sampling points of the entire watershed and (ii) those located in tributaries with catchment areas of less than 20 km², respectively (Table S1). In the tributary model, the $\delta^{18}O_{PO_4}$ level is likely determined primarily by the source isotopic signatures because of the short P transport distance (travel time) and hindering biological P uptake due to the relatively low light intensity in forest streams[6,36] of our study area, although the biological uptake differs on the basis of the headwater characteristics, such as relative benthic area to water volume and connectivity with the riparian and hyporheic zones.[22] In the watershed model, by contrast, we expect the $\delta^{18}O_{PO_4}$ values to be modified by the cumulative effects of metabolic processes due to a longer travel time for P along the river course. For each of these two models, the best fit was selected from all possible combinations of the explanatory variables based on Akaike's information criterion (AIC) to minimize the information and variance inflation factor (VIF) to avoid multicollinearity (criterion: VIF < 10). The statistical analyses were conducted using R version 3.4.4.[37]

Prior to isoscape mapping, 489 points including the actual sampling points were set along the river on the GIS map, whereupon the watershed characteristics of land cover and lithological type were analyzed for each point as mentioned above. The $\delta^{18}O_{PO_4}$ value at each point was predicted using the best fits for the watershed and tributary models. To project the isoscape maps, we interpolated the predicted values of $\delta^{18}O_{PO_4}$ spatially for the entire river system using the inverse distance weighting (IDW) tool of ArcGIS to take the inverse-distance-weighted average between neighborhood points.

3.0. RESULTS AND DISCUSSION

3.1. $\delta^{18}O_{PO_4}$ Values in River Water. Although we collected river water from 30 sites in the Yasu River, we obtained a sufficient amount of Ag_3PO_4 for $\delta^{18}O_{PO_4}$ analysis from only half the samples (N = 15). This may be attributed to the very low orthophosphate concentrations in the samples that did not yield sufficient Ag_3PO_4. Prior to our synoptic sampling, we calculated the water volume needed for $\delta^{18}O_{PO_4}$ analysis based on a preliminary survey of the SRP

concentrations at each site. Nevertheless, this estimate was higher than the Pi in the samples; it is known that SRP measured by the molybdenum-blue method includes P species other than orthophosphate,[38] explaining this overestimation. Recently, Maruo et al.[39] reported that the ratio of orthophosphate to SRP in river and lake water samples collected from the Lake Biwa Watershed varied widely from 0.06 to 0.79, requiring more than 10 times the volume of water we collected to obtain enough Ag_3PO_4. Accordingly, it is recommended that water samples of volume much larger than needed be collected for the $\delta^{18}O_{PO_4}$ analysis,[7] assuming that the freshwater samples have a low orthophosphate-to-SRP ratio.

Within the Yasu River Watershed, the $\delta^{18}O_{PO_4}$ values of dissolved Pi in river water that could be measured ranged from 10.3‰ to 17.6‰ (Figure 2). Similarly large variations have
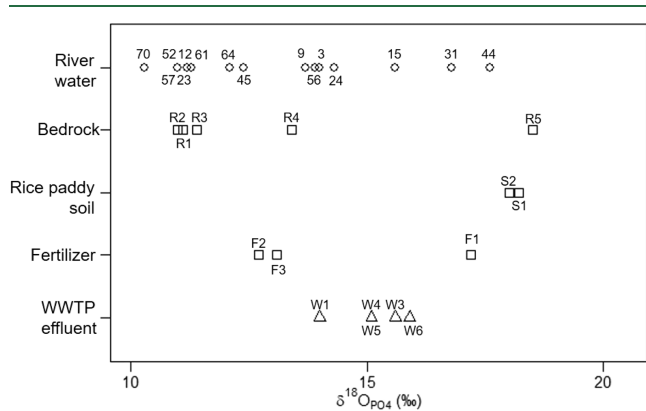

Figure 2. $\delta^{18}O_{PO_4}$ values in Yasu River water and P source samples collected within Yasu River Watershed, including bedrock, rice paddy soil, fertilizer, and wastewater treatment plant (WWTP) effluents. Numbers on symbols refer to sampling sites as shown in Figure 1.

been observed in other coastal and freshwater systems,[9] in which P sources and P metabolic processes are expected to have high spatiotemporal variability. For example, the $\delta^{18}O_{PO_4}$ values dissolved Pi in watersheds around Lake Erie span 4.7‰, in the San Joaquin River System 7.2‰, and in the Lake Tahoe watershed 3.0‰.[40] By contrast, in the catchment of the River Taw in southwest England, the $\delta^{18}O_{PO_4}$ values of dissolved Pi in river water vary by only 1.7‰ along the main channel from upstream to downstream sites.[17] The $\delta^{18}O_{PO_4}$ values for the water in the River Taw catchment are similar to those expected from theoretical equilibrium at all sites and differ from those of potential natural and anthropogenic P sources, suggesting that in this river the source isotope signatures are overwritten by in-stream biological processes.

In the YRW, the $\delta^{18}O_{PO_4}$ values of dissolved Pi deviate greatly from the $\delta^{18}O_{PO_4Eq}$ for many tributary streams (Figure S2), indicating that phosphate ions in the river water are not being taken up fully by the living biomass in the streams and these values can be utilized for identifying P source in the watershed. The rate of biological P recycling depends on stream characteristics such as biological activity, nutrient balance, and travel time.[6,17,19,41] We surmise the relatively small catchment area (387 km²), steep gradient (87−1213 m in elevation) and high flow velocity (0.79 ± 0.62 km/h; Table S1) of the Yasu River may result in a travel time that is too

short for complete in-stream microbial P turnover.[6,36] Consequently, the Yasu River has a wide range of $\delta^{18}O_{PO_4}$ values imprinted by isotope signatures derived from various P sources that dominate different sections of the watershed.

3.2. $\delta^{18}O_{PO_4}$ Values in Natural and Anthropogenic P Sources.
Our source samples have distinct $\delta^{18}O_{PO_4}$ values (Figure 2), allowing us to examine the relative importance of each source to the river. According to previous studies, $\delta^{18}O_{PO_4}$ values in source samples vary widely, covering all the range of our source sample (details are shown below).[7−10]

3.2.1. Bedrock and Forest-Floor Soils.
The $\delta^{18}O_{PO_4}$ values of HCl extractable Pi in bedrock differs based on rock type (Figure 2 and Table S4). The granite rocks (R3 and R4) found in the upstream mountain area and within the watershed of some of the first-order streams in the lower catchment (Figure 1) have the $\delta^{18}O_{PO_4}$ value range of 11.4−13.4‰, whereas the sedimentary rock value is 18.5‰ (R5) (Figure 2 and Table S4). The extracted bedrock Pi using 1 M HCl mainly constitutes the calcium-bound P fraction (e.g., apatite).[31] Apatite in plutonic rocks generally has low $\delta^{18}O_{PO_4}$ values (6.0−13.5‰),[42−44] which are similar to the granite $\delta^{18}O_{PO_4}$ values observed in the YRW. By contrast, because $\delta^{18}O_{PO_4}$ values in biotic apatite are determined from the $\delta^{18}O_{H_2O}$ values of ambient water and the temperature during apatite formation, sedimentary apatite shows great variation with rock age and location (6.0−25.0‰).[14,45] Our sedimentary rock value is consistent with those of biotic apatite. The accretionary complex comprises a mixture of igneous and biotic apatite; thus, the $\delta^{18}O_{PO_4}$ values of HCl extractable Pi in the accretionary complex (11.0−11.1‰) are controlled by the relative contribution of these rock types.

In the present study, we were unable to characterize the $\delta^{18}O_{PO_4}$ values of $NaHCO_3$ extractable Pi in the forest-floor soils. Japanese forest soils typically have low labile Pi concentrations (Table S4) and high organic-matter content,[46] preventing $\delta^{18}O_{PO_4}$ analysis.[47,48] According to previous studies, the $\delta^{18}O_{PO_4}$ values in soil samples vary between different operationally defined soil fractions.[8,29,48−50] In natural systems, the $\delta^{18}O_{PO_4}$ values of labile and less labile P fractions are typically close to that expected at the isotopic equilibrium with water and that of the parent rock material, respectively,[29,49,50] although this phenomenon is not always the case and actual values also depend on pedogenesis processes, such as weathering rate and biological activity.[51,52] If the former case (i.e., equilibrium) applies to our study area, then the $\delta^{18}O_{PO_4Eq}$ values of labile Pi in forest soils are estimated to be around 15.3‰ based on the average $\delta^{18}O_{H_2O}$ (−6.41‰) and the air temperature (18 °C) in the upper catchment (Tsuchiyama) during the sampling period. This value differs from that of $\delta^{18}O_{PO_4}$, which we measured for accretionary complex and granite rock. Therefore, forest soil is possibly the source with a wide value range of $\delta^{18}O_{PO_4}$ to the river.

3.2.2. Fertilizers and Rice Paddy Soils.
In our analysis, the $\delta^{18}O_{PO_4}$ values of water-soluble P in chemical and organic fertilizers differ (Figure 2 and Table S4), which may depend on the raw material of phosphate used to produce the fertilizer. Previous studies reported that manufactured fertilizers show a

Table 1. Multiple-Regression Statistics for the Best Fits of the Watershed and Tributary Models Based on AIC[a]

	variable	coefficient	SE	p	VIF	R^2
watershed model	intercept	10.0	1.40	0.001		
	accretionary complex	−3.18	1.36	0.04	1.5	
	forest	3.40	1.77	0.08	2.0	0.69
	rice paddy	11.1	3.17	0.01	1.7	
tributary model	intercept	10.5	0.68	0.001		
	accretionary complex	−11.2	1.75	0.001	8.4	
	granite	−8.05	1.76	0.01	9.9	0.96
	forest	11.3	1.81	0.002	7.8	
	rice paddy	5.60	2.06	0.04	2.7	

[a]VIF, variance inflation factor. See text for details of the two models.
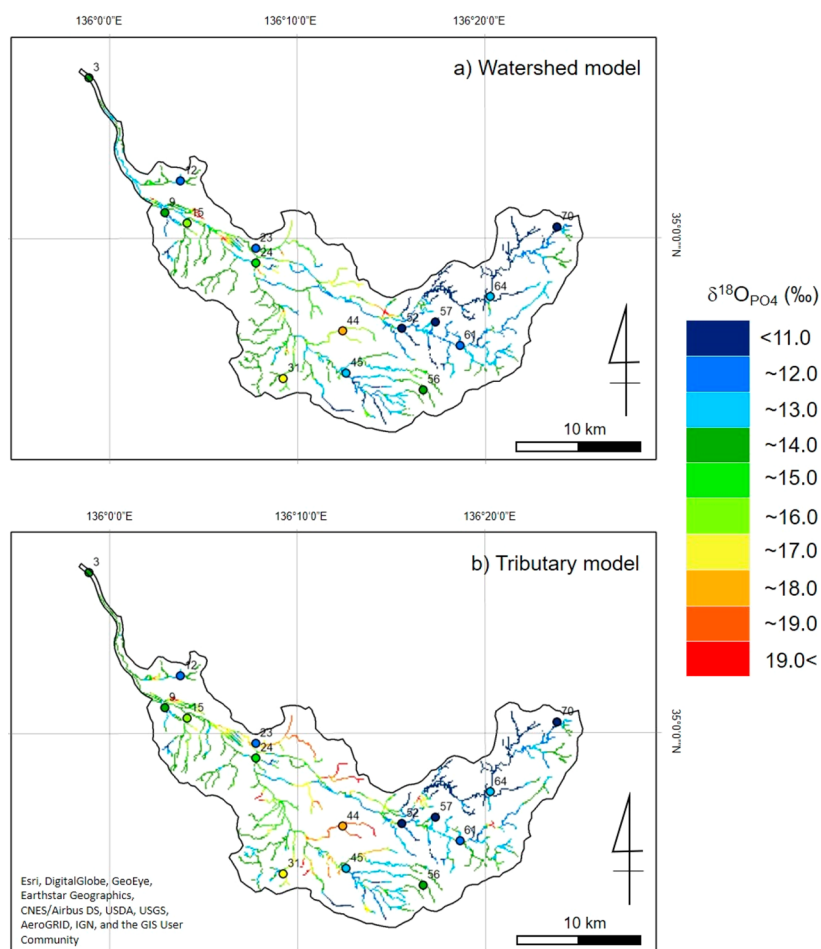
Figure 3. Isoscapes of river water $\delta^{18}O_{PO_4}$ based on (a) watershed model and (b) tributary model. Colored circles and numbers refer to the observed $\delta^{18}O_{PO_4}$ values in the river water and sampling sites. See text for details of the two models.

wide range of $\delta^{18}O_{PO_4}$ values (15.5−27.0‰), reflecting the isotopic signatures of the phosphate ores used in production.[10,40,53] Our chemical-fertilizer sample (F2, 12.7‰) had a $\delta^{18}O_{PO_4}$ signature similar to that of its stock solution (F3, 13.1‰), which is used for many manufactured products that have a large market share in Shiga Prefecture. A value of 12−13‰ can therefore be regarded as representative isotopic signature that is characteristic of chemical fertilizers in the YRW.

The $\delta^{18}O_{PO_4}$ values of $NaHCO_3$ extractable Pi in rice paddy soil samples collected at two different places during the nonirrigation period had almost the same values (18.0−

18.2‰) (Figure 2 and Table S4). These values may be controlled by fertilizer addition and/or biological recycling. These values are similar to that of the organic fertilizer value (F1, 17.2‰), although they differ from that of the chemical fertilizer (Figure 2 and Table S4). One possibility is that the organic fertilizer sets the $\delta^{18}O_{PO_4}$ values of $NaHCO_3$ extractable Pi in the paddy soils. Another explanation is that the biological recycling of labile Pi derived from fertilizers in rice paddies determines the paddy soil signature. A previous study reported that the $\delta^{18}O_{PO_4}$ values of labile Pi in irrigated soils rapidly approach an equilibrium value within half a month of adding P fertilizers, thus overwriting the source isotope

signatures.[54,55] Therefore, the $\delta^{18}O_{PO_4}$ values of $NaHCO_3$ extractable Pi in rice paddy soils may depend on the seasonality in water temperature and $\delta^{18}O_{H_2O}$. We estimated the equilibrium value expected in the sampling period based on our monitoring data of $\delta^{18}O_{H_2O}$ ($-3.46 \pm 1.05\%o$) and the water temperature (20.9 ± 4.8 °C) of the irrigated water in the rice paddies during sampling period. The resulting $\delta^{18}O_{PO_4Eq}$ value is $17.6\%o$. If indeed Pi in rice paddies is almost completely recycled, then the observed $\delta^{18}O_{PO_4}$ in river water was derived from rice paddy wastewater flowing to the river through agricultural drainage canals or culverts.

3.2.3. WWTP Effluents. The $\delta^{18}O_{PO_4}$ values of dissolved Pi in the wastewater treatment plant (WWTP) effluents are relatively constrained, spanning a narrow range (Figure 2), suggesting that these isotopic signatures are typical of the WWTP effluents in this watershed. Effluents from WWTPs are often considered to be the primary point sources of domestic P in a river.[18,19] In the entire LBW, the point sources from the WWTPs account for 16.1% of the total P loading into the lake basin.[28] To estimate the contribution of the WWTP-derived P discharged into the tributaries of the Yasu River, we calculated the P load from each small-scale WWTP using the maximum discharge and SRP concentration of its effluent. The estimated P load ranged from 8.85 to 63.6 mmol/day, which is large enough to alter the $\delta^{18}O_{PO_4}$ values of dissolved Pi in the river water in small tributaries (Table S2). However, even for a site in a small tributary (site 44) that is located immediately downstream from a small-scale WWTP (Figure 1a), the $\delta^{18}O_{PO_4}$ value of dissolved Pi in the river water ($17.6\%o$) differs markedly from that in the WWTP effluent ($14.0-15.9\%o$) (Tables S2 and S3). This result differs from reported conditions in the River Beult in the United Kingdom, in which the $\delta^{18}O_{PO_4}$ values of dissolved Pi in the river downstream from a WWTP were found to be similar to those of the WWTP effluents.[18] In our case, intermittent discharge from WWTP may result in the difference between the $\delta^{18}O_{PO_4}$ value in WWTP effluent and downstream tributary water. Thus, the actual $\delta^{18}O_{PO_4}$ values of dissolved Pi in the downstream tributary water should show large temporal variation depending on the discharge times and rates from the WWTPs.

Considering that the river discharge in the main stream is much greater than water volumes added by the small-scale WWTP effluent disposal, the WWTP-derived P may be diluted substantially with river water in the lower catchment. The fact that effluent from the large WWTP that serves more than 90% of the watershed population is not discharged directly into the Yasu River suggests that the impact of the WWTPs on the $\delta^{18}O_{PO_4}$ values of dissolved Pi in the river water is not great overall.

3.3. $\delta^{18}O_{PO_4}$ Isoscapes. The watershed and tributary models for $\delta^{18}O_{PO_4}$ isoscapes account for 69% and 96% of the spatial variation in the $\delta^{18}O_{PO_4}$ values dissolved Pi in the river water, respectively. These values are sufficiently high when constructing an isoscape map (Table 1).[31] The best-fit model of the $\delta^{18}O_{PO_4}$ isoscapes is the one that uses the proportional areas of rice paddy, forest, and accretionary complex as explanatory variables to be employed as predictors for the watershed model and that of granite and the same predictors of the watershed model for the tributary model. The isoscape maps of the $\delta^{18}O_{PO_4}$ values of dissolved Pi in the river water, based on two models, exhibit a similar trend (Figure 3), that is, low value in the upstream and average−high value in the middle and downstream.

Although the predicted values using the two models significantly correlated with each other (Pearson's $r = 0.73$; $p < 0.05$), the average and SD of the predicted values from the tributary model ($13.6 \pm 2.6\%o$) were significantly higher than that from the watershed model ($12.8 \pm 2.0\%o$) ($p < 0.05$; t test for average and F test for SD). The differences in averages, SDs, and R^2 values of the two models may be caused by isotope fractionation associated with microbial P turnover particularly in the lower stream. Because small tributaries in the upper catchments are expected to have low microbial P turnover due to low forest canopy openness (0.36 ± 0.22, Table S1) and high flow velocity (Table S1),[6,36] the source isotope signatures are dominant in the Pi pool of these streams. Meanwhile, the main stream in the lower catchment has a long travel time for P in open water, thereby cumulatively enhancing the biological P recycling during its downward movement. These differences may affect model predictions and result in the lower R^2 value for the watershed model. Hence, future work will involve incorporating in-stream biological processes into the models to fully understand the P dynamics in the entire watershed.

Nonpoint agricultural loads have been regarded as a major P source (16.0%) similar to the contributions from WWTPs (16.1%) and septic tanks (15.5%) based on a simulation model for the annual total P loads from LBW watershed into Lake Biwa in 2015.[28] In addition, the P loads from rice paddies during the irrigation period (4.82 kgP ha^{-1} day^{-1}) was estimated to be 2.6 times higher than that in the nonirrigation period (1.86 kgP ha^{-1} day^{-1}).[28] Therefore, the P loads from the rice paddies are expected to be the highest P source during irrigation period. Indeed, in our study, the river reach with high $\delta^{18}O_{PO_4}$ values corresponds to areas dominated by rice paddies that are situated on sedimentary rocks (Figures 1 and 3 and Table S5). Moreover, the proportional area of rice paddies shows the strongest positive correlation with the river water $\delta^{18}O_{PO_4}$ among the land cover and lithological types (Figures S3 and S4). In the rice paddies, chemical fertilizer is expected to be the major inorganic P source because of its use in high concentrations and its lability (Table S4); however, the $\delta^{18}O_{PO_4}$ value of the fertilizer phosphate is much lower than that observed in streamwater even where the proportional area of rice paddies is high (Figure S3a). The $\delta^{18}O_{PO_4}$ values of dissolved Pi in the river water are similar to those of organic fertilizer, rice paddy soils, and sedimentary rocks, which have similar signatures. We suggest that in the rice paddies, most of the labile Pi from fertilizer application is turned over during the irrigation period, effectively erasing the source signature, as discussed in section 3.2.2. Taken together, the P derived from sedimentary rock and biologically recycled P are likely to be the dominant nonpoint P sources to the river water in areas adjacent to the rice paddies.

Because the forest streams in our study area have few anthropogenic P sources (and low SRP concentrations), we expect natural P sources such as bedrocks and forest soils to make a relatively large contribution in forest streams. Indeed,

the isoscapes show low $\delta^{18}O_{PO_4}$ values of dissolved Pi in the upstream reaches of the river, where forest developed on accretionary complex and granite bedrock is abundant (Figures 1 and 3 and Table S5). The proportional area of forest is not correlated significantly with the $\delta^{18}O_{PO_4}$ value of dissolved Pi in river water (Figure S3c); instead, the $\delta^{18}O_{PO_4}$ values show a tendency to converge to that of granite and accretionary complex bedrock. This result indicates that bedrock and/or P pools in forest soils, with $\delta^{18}O_{PO_4}$ value reflecting that of bedrock,[29,49,50] are the dominant P sources in the forested areas.

We successfully demonstrated that the $\delta^{18}O_{PO_4}$ isoscape models are promising tools for assessing nonpoint sources of anthropogenic and natural P loadings into a watershed because potential sources, such as land cover and lithological type, had distinct $\delta^{18}O_{PO_4}$ values. However, we also had a limitation on the precision of the estimation in the watershed scale because the isoscapes herein are based on a small data set of $\delta^{18}O_{PO_4}$ values. Therefore, in future studies, obtaining additional $\delta^{18}O_{PO_4}$ data of river water and P sources is important to improve the model. We also need to consider and include additional factors affecting the $\delta^{18}O_{PO_4}$ value in river water, such as existence of additional P sources (e.g., bank erosion, atmospheric deposition, internal loads from river sediment, and seasonal change in P loads from each P source). In addition, complementing the isoscape models by using other independent methods, such as synoptic monitoring and hydrological models, is probably necessary. The isoscape approach should be applicable in watersheds with characteristics similar to that of our watershed and useful for watershed management, wherein excellent practices are designed to reduce the P loads to control cultural eutrophication in river and lake ecosystems.

ASSOCIATED CONTENT

Ⓢ Supporting Information

The Supporting Information is available free of charge on the ACS Publications website at DOI: 10.1021/acs.est.8b05837.

Text S1, Figures S1−S4, and Tables S1−S5 (PDF)

AUTHOR INFORMATION

Corresponding Author

*Phone: +81-75-707-2285; e-mail: tishida@chikyu.ac.jp.

ORCID Ⓞ

Takuya Ishida: 0000-0003-3290-4840
Jun'ichiro Ide: 0000-0002-0992-7318

Notes

The authors declare no competing financial interest.

ACKNOWLEDGMENTS

ABBREVIATIONS

AIC	Akaike's information criterion
IDW	inverse distance weighting
IRMS	isotope-ratio mass-spectrometer
JA	Japan Agricultural Cooperatives
LBW	Lake Biwa Watershed
P	phosphorus
Pi	inorganic phosphate
RIHN	Research Institute for Humanity and Nature
SRP	soluble reactive phosphate
UPW	ultrapure water
VIF	variance inflation factor
YRW	Yasu River Watershed
VSMOW	Vienna standard mean ocean water
YRW	Yasu River Watershed
WWTP	wastewater treatment plant

REFERENCES

(1) Yoon, S. W.; Chung, S. W.; Oh, D. G.; Lee, J. W. Monitoring of Non-Point Source Pollutants Load from a Mixed Forest Land Use. *J. Environ. Sci.* **2010**, *22* (6), 801−805.

(2) Dove, A.; Chapra, S. C. Long-Term Trends of Nutrients and Trophic Response Variables for the Great Lakes. *Limnol. Oceanogr.* **2015**, *60* (2), 696−721.

(3) Boesch, D. F.; Brinsfield, R. B.; Magnien, R. E. Chesapeake Bay Eutrophication: Scientific Understanding, Ecosystem Restoration, and Challenges for Agriculture. *J. Environ. Qual.* **2001**, *30* (2), 303−320.

(4) Aciego, S. M.; Riebe, C. S.; Hart, S. C.; Blakowski, M. A.; Carey, C. J.; Aarons, S. M.; Dove, N. C.; Botthoff, J. K.; Sims, K. W. W.; Aronson, E. L. Dust Outpaces Bedrock in Nutrient Supply to Montane Forest Ecosystems. *Nat. Commun.* **2017**, *8*, 14800.

(5) Kagatsume, T. Water Conservation Policy of Shiga Prefectural Government. In *Lake Biwa: Interactions between Nature and People*; Kawanabe, H., Nishino, M., Maehata, M., Eds.; Springer Netherlands: Dordrecht, 2012; pp 423−427.

(6) Tonderski, K.; Andersson, L.; Lindström, G.; St Cyr, R.; Schönberg, R.; Taubald, H. Assessing the Use of $\delta^{18}O$ in Phosphate as a Tracer for Catchment Phosphorus Sources. *Sci. Total Environ.* **2017**, *607−608*, 1−10.

(7) Paytan, A.; McLaughlin, K. Tracing the Sources and Biogeochemical Cycling of Phosphorus in Aquatic Systems Using Isotopes of Oxygen in Phosphate. In *Handbook of Environmental Isotope Geochemistry*; Baskaran, M., Ed.; Springer: Berlin, 2012; Vol. *I*, pp 419−436.

(8) Tamburini, F.; Pfahler, V.; von Sperber, C.; Frossard, E.; Bernasconi, S. M. Oxygen Isotopes for Unraveling Phosphorus Transformations in the Soil−Plant System: A Review. *Soil Sci. Soc. Am. J.* **2014**, *78*, 38−46.

(9) Davies, C. L.; Surridge, B. W. J.; Gooddy, D. C. Phosphate Oxygen Isotopes within Aquatic Ecosystems: Global Data Synthesis and Future Research Priorities. *Sci. Total Environ.* **2014**, *496*, 563−575.

(10) McLaughlin, K.; Young, M.; Paytan, A.; Kendall, C. The Oxygen Isotopic Composition of Phosphate: A Tracer for Phosphate Sources and Cycling. In *Application of Isotope Techniques for Assessing Nutrient Dynamics in River Basins*; 2013; pp 93−110.

(11) Liang, Y.; Blake, R. E. Oxygen Isotope Signature of Pi Regeneration from Organic Compounds by Phosphomonoesterases and Photooxidation. *Geochim. Cosmochim. Acta* **2006**, *70* (15), 3957−3969.

(12) Liang, Y.; Blake, R. E. Oxygen Isotope Composition of Phosphate in Organic Compounds: Isotope Effects of Extraction Methods. *Org. Geochem.* **2006**, *37* (10), 1263−1277.

(13) Liang, Y.; Blake, R. E. Compound- and Enzyme-Specific Phosphodiester Hydrolysis Mechanisms Revealed by $\delta^{18}O$ of Dissolved Inorganic Phosphate: Implications for Marine P Cycling. *Geochim. Cosmochim. Acta* **2009**, *73* (13), 3782−3794.

(14) Longinelli, A.; Nuti, S. Revised Phosphate-Water Isotopic Temperature Scale. *Earth Planet. Sci. Lett.* **1973**, *19* (3), 373−376.

(15) Chang, S. J.; Blake, R. E. Precise Calibration of Equilibrium Oxygen Isotope Fractionations between Dissolved Phosphate and Water from 3 to 37°C. *Geochim. Cosmochim. Acta* **2015**, *150*, 314−329.

(16) Blake, R. E.; O'Neil, J. R.; Surkov, A. V. Biogeochemical Cycling of Phosphorus: Insights from Oxygen Isotope Effects of Phosphoenzymes. *Am. J. Sci.* **2005**, *305* (6−8), 596−620.

(17) Granger, S. J.; Heaton, T. H. E.; Pfahler, V.; Blackwell, M. S. A.; Yuan, H.; Collins, A. L. The Oxygen Isotopic Composition of Phosphate in River Water and Its Potential Sources in the Upper River Taw Catchment, UK. *Sci. Total Environ.* **2017**, *574*, 680−690.

(18) Gooddy, D. C.; Lapworth, D. J.; Bennett, S. A.; Heaton, T. H. E.; Williams, P. J.; Surridge, B. W. J. A Multi-Stable Isotope Framework to Understand Eutrophication in Aquatic Ecosystems. *Water Res.* **2016**, *88*, 623−633.

(19) Pistocchi, C.; Tamburini, F.; Gruau, G.; Ferhi, A.; Trevisan, D.; Dorioz, J.-M. Tracing the Sources and Cycling of Phosphorus in River Sediments Using Oxygen Isotopes: Methodological Adaptations and First Results from a Case Study in France. *Water Res.* **2017**, *111*, 346−356.

(20) McLaughlin, K.; Cade-Menun, B. J.; Paytan, A. The Oxygen Isotopic Composition of Phosphate in Elkhorn Slough, California: A Tracer for Phosphate Sources. *Estuarine, Coastal Shelf Sci.* **2006**, *70* (3), 499−506.

(21) McLaughlin, K.; Kendall, C.; Silva, S. R.; Young, M.; Paytan, A. Phosphate Oxygen Isotope Ratios as a Tracer for Sources and Cycling of Phosphate in North San Francisco Bay, California. *J. Geophys. Res.* **2006**, *111*, 1.

(22) Riley, W. D.; Potter, E. C. E.; Biggs, J.; Collins, A. L.; Jarvie, H. P.; Jones, J. I.; Kelly-Quinn, M.; Ormerod, S. J.; Sear, D. A.; Wilby, R. L.; et al. Small Water Bodies in Great Britain and Ireland: Ecosystem Function, Human-Generated Degradation, and Options for Restorative Action. *Sci. Total Environ.* **2018**, *645*, 1598−1616.

(23) Li, X.; Wang, Y.; Stern, J.; Gu, B. Isotopic Evidence for the Source and Fate of Phosphorus in Everglades Wetland Ecosystems. *Appl. Geochem.* **2011**, *26* (5), 688−695.

(24) Allen, S. T.; Kirchner, J. W.; Goldsmith, G. R. Predicting Spatial Patterns in Precipitation Isotope ($\delta^{2}H$ and $\delta^{18}O$) Seasonality Using Sinusoidal Isoscapes. *Geophys. Res. Lett.* **2018**, *45*, 4859−4868.

(25) Kendall, C.; Coplen, T. B. Distribution of Oxygen-18 and Deuteriun in River Waters across the United States. *Hydrol. Processes* **2001**, *15* (7), 1363−1393.

(26) Bowen, G.; Isoscapes, J. Spatial Pattern in Isotopic Biogeochemistry. *Annu. Rev. Earth Planet. Sci.* **2010**, *38* (1), 161−187.

(27) Shiga Prefecture Department of Lake Biwa and the Environment. *Sewage Work of Shiga Prefecture*; 2017.

(28) Lake Biwa Environmental Reseach Institute. *Simulation for Future Water Quality Prediction Related to "7th Phase of Lake Water Quality Conservation Plan"*; 2018.

(29) Angert, A.; Weiner, T.; Mazeh, S.; Sternberg, M. Soil Phosphate Stable Oxygen Isotopes across Rainfall and Bedrock Gradients. *Environ. Sci. Technol.* **2012**, *46* (4), 2156−2162.

(30) McLaughlin, K.; Silva, S.; Kendall, C.; Stuart-Williams, H.; Paytan, A. A Precise Method for the Analysis of $\delta^{18}O$ of Dissolved Inorganic Phosphate in Seawater. *Limnol. Oceanogr.: Methods* **2004**, *2*, 202−212.

(31) Hedley, M. J.; Stewart, J. W. B.; Chauhan, B. S. Changes in Inorganic and Organic Soil Phosphorus Fractions Induced by Cultivation Practices and by Laboratory Incubations1. *Soil Sci. Soc. Am. J.* **1982**, *46* (5), 970.

(32) Turner, B. L.; Haygarth, P. M. Changes in Bicarbonate-Extractable Inorganic and Organic Phosphorus by Drying Pasture Soils. *Soil Sci. Soc. Am. J.* **2003**, *67* (1), 344−350.

(33) Jiang, Z. H.; Zhang, H.; Jaisi, D. P.; Blake, R. E.; Zheng, A. R.; Chen, M.; Zhang, X. G.; Peng, A. G.; Lei, X. T.; Kang, K. Q.; et al. The Effect of Sample Treatments on the Oxygen Isotopic Composition of Phosphate Pools in Soils. *Chem. Geol.* **2017**, *474* (May), 9−16.

(34) Murphy, J.; Riley, J. P. A Modified Single Solution Method for the Determination of Phosphate in Natural Waters. *Anal. Chim. Acta* **1962**, *27*, 31−36.

(35) Mellett, T.; Selvin, C.; Defforey, D.; Roberts, K.; Lecher, A. L.; Dennis, K.; Gutknecht, J.; Field, C.; Paytan, A. Assessing Cumulative Effects of Climate Change Manipulations on Phosphorus Limitation in a Californian Grassland. *Environ. Sci. Technol.* **2018**, *52* (1), 98−106.

(36) Hill, W. R.; Mulholland, P. J.; Marzolf, E. R. Stream Ecosystem Responses to Forest Leaf Emergence in Spring. *Ecology* **2001**, *82* (8), 2306−2319.

(37) R Core Team. A Language and Environment for Statistical Computing. R Foundation for Statistical Computing: Vienna, Austria, 2018.

(38) Karl, D. M.; Tien, G. MAGIC: A Sensitive and Precise Method for Measuring Dissolved Phosphorus in Aquatic Environments. *Limnol. Oceanogr.* **1992**, *37* (1), 105−116.

(39) Maruo, M.; Ishimaru, M.; Azumi, Y.; Kawasumi, Y.; Nagafuchi, O.; Obata, H. Comparison of Soluble Reactive Phosphorus and Orthophosphate Concentrations in River Waters. *Limnology* **2016**, *17* (1), 7−12.

(40) Young, M. B.; McLaughlin, K.; Kendall, C.; Stringfellow, W.; Rollog, M.; Elsbury, K.; Donald, E.; Paytan, A. Characterizing the Oxygen Isotopic Composition of Phosphate Sources to Aquatic Ecosystems. *Environ. Sci. Technol.* **2009**, *43* (14), 5190−5196.

(41) Hoellein, T. J.; Tank, J. L.; Rosi-Marshall, E. J.; Entrekin, S. A.; Lamberti, G. A. Controls on Spatial and Temporal Variation of Nutrient Uptake in Three Michigan Headwater Streams. *Limnol. Oceanogr.* **2007**, *52* (5), 1964−1977.

(42) Burmann, F.; Keim, M. F.; Oelmann, Y.; Teiber, H.; Marks, M. A. W.; Markl, G. The Source of Phosphate in the Oxidation Zone of Ore Deposits: Evidence from Oxygen Isotope Compositions of Pyromorphite. *Geochim. Cosmochim. Acta* **2013**, *123*, 427−439.

(43) Markel, D.; Kolodny, Y.; Luz, B.; Nishri, A. Phosphorus Cycling and Phosphorus Sources in Lake Kinneret: Traving by Oxygen Isotopes in Phosphate. *Isr. J. Earth Sci.* **1994**, *43*, 165−178.

(44) Blake, R. E.; Chang, S. J.; Lepland, A. Phosphate Oxygen Isotopic Evidence for a Temperate and Biologically Active Archaean Ocean. *Nature* **2010**, *464* (7291), 1029−1032.

(45) Kolodny, Y.; Luz, B.; Navon, O. Oxygen Isotope Variations in Phosphate of Biogenic Apatites, I. Fish Bone Apatite—rechecking the Rules of the Game. *Earth Planet. Sci. Lett.* **1983**, *64* (3), 398−404.

(46) Morisada, K.; Ono, K.; Kanomata, H. Organic Carbon Stock in Forest Soils in Japan. *Geoderma* **2004**, *119* (1−2), 21−32.

(47) Tamburini, F.; Bernasconi, S. M.; Angert, A.; Weiner, T.; Frossard, E. A Method for the Analysis of the $\delta^{18}O$ of Inorganic Phosphate Extracted from Soils with HCl. *Eur. J. Soil Sci.* **2010**, *61* (6), 1025−1032.

(48) Zohar, I.; Shaviv, A.; Klass, T.; Roberts, K.; Paytan, A. Method for the Analysis of Oxygen Isotopic Composition of Soil Phosphate Fractions. *Environ. Sci. Technol.* **2010**, *44* (19), 7583−7588.

(49) Tamburini, F.; Pfahler, V.; Bünemann, E. K.; Guelland, K.; Bernasconi, S. M.; Frossard, E. Oxygen Isotopes Unravel the Role of Microorganisms in Phosphate Cycling in Soils. *Environ. Sci. Technol.* **2012**, *46* (11), 5956−5962.

(50) Roberts, K.; Defforey, D.; Turner, B. L.; Condron, L. M.; Peek, S.; Silva, S.; Kendall, C.; Paytan, A. Oxygen Isotopes of Phosphate and Soil Phosphorus Cycling across a 6500year Chronosequence under Lowland Temperate Rainforest. *Geoderma* **2015**, *257−258*, 14−21.

(51) Helfenstein, J.; Tamburini, F.; von Sperber, C.; Massey, M. S.; Pistocchi, C.; Chadwick, O. A.; Vitousek, P. M.; Kretzschmar, R.; Frossard, E. Combining Spectroscopic and Isotopic Techniques Gives a Dynamic View of Phosphorus Cycling in Soil. *Nat. Commun.* **2018**, *9* (1), 3226.

(52) Pfahler, V.; Tamburini, F.; Bernasconi, S. M.; Frossard, E. A Dual Isotopic Approach Using Radioactive Phosphorus and the Isotopic Composition of Oxygen Associated to Phosphorus to Understand Plant Reaction to a Change in P Nutrition. *Plant Methods* **2017**, *13* (1), 1−12.

(53) Gruau, G.; Legeas, M.; Riou, C.; Gallacier, E.; Martineau, F.; Hénin, O. The Oxygen Isotope Composition of Dissolved Anthropogenic Phosphates: A New Tool for Eutrophication Research? *Water Res.* **2005**, *39* (1), 232−238.

(54) Zohar, I.; Shaviv, A.; Young, M.; Kendall, C.; Silva, S.; Paytan, A. Phosphorus Dynamics in Soils Irrigated with Reclaimed Waste Water or Fresh Water - A Study Using Oxygen Isotopic Composition of Phosphate. *Geoderma* **2010**, *159* (1−2), 109−121.

(55) Gross, A.; Angert, A. What Processes Control the Oxygen Isotopes of Soil Bio-Available Phosphate? *Geochim. Cosmochim. Acta* **2015**, *159*, 100−111.

Supporting Information

Identification of Phosphorus Sources in a Watershed Using a Phosphate Oxygen Isoscape Approach

Takuya Ishida*,[1] Yoshitoshi Uehara,[1] Tomoya Iwata,[2] Abigail P. Cid-Andres,[3] Satoshi Asano,[4] Tohru Ikeya,[1] Ken'ichi Osaka,[5] Jun'ichiro Ide,[6] Osbert Leo A. Privaldos,[7] Irisse Bianca B. De Jesus,[8] Elfritzson M. Peralta,[8] Ellis Mika C. Triño,[8] Chia-Ying Ko,[9] Adina Paytan,[10] Ichiro Tayasu,[1] Noboru Okuda[1]

[1]Research Institute for Humanity and Nature, 457-4, Motoyama, Kamigamo, Kyoto, 603-8047, Japan

[2]Faculty of Life and Environmental Science, University of Yamanashi, 4-4-37, Takeda, Kofu, Yamanashi 400-8510, Japan

[3]Department of Physical Sciences, College of Science, Polytechnic University of the Philippines, Anonas Street. Sta. Mesa, Manila, 1016, Philippines

[4]Lake Biwa Environment Research Institute 5-34, Yanagasaki, Ohtsu, Shiga, 520-0022, Japan

[5]School of Environmental Sciences, The University of Shiga Prefecture, 2500, Hasaka, Hikone, Shiga, 522-8533, Japan

[6]Institute of Decision Science for a Sustainable Society, Kyushu University, 394, Tsubakuro, Sasaguri, Fukuoka, 811-2415, Japan

[7]Laguna Lake Development Authority, National Ecology Center, East Avenue, Diliman, Quezon City, 1101, Philippines

[8]The Graduate School, University of Santo Tomas, España Boulevard, Manila, 1015, Philippines

[9]Institute of Fisheries Science & Department of Life Science, National Taiwan University, No. 1, Sec. 4, Roosevelt Rd., Taipei 10617, Taiwan

[10]Institute of Marine Sciences University of California Santa Cruz, 1156, High Street, Santa Cruz, CA, 95064, USA

*Corresponding Author:

Takuya Ishida: tishida@chikyu.ac.jp; +81-75-707-2285

This supporting information contains:

Text S1, Figure S1-S4, and Table S1-S5

Text S1. Wastewater treatment plants (WWTPs) in the Yasu River Watershed (YRW).

As described in Section 2.1, almost all domestic wastewater in this catchment (91.4% of the human population in five local government areas, including YRW) is treated in one large WWTP. This WWTP treats approximately 43,000 $m^3 \cdot day^{-1}$ wastewater and discharges into the nearby lake basin, but not affecting the Yasu River. A small-scale WWTP, which is located in a rural area, serves 4.6% of human population directly into the nearby stream tributaries of the Yasu River. These WWTPs treat less than 550 $m^3 \cdot day^{-1}$ wastewater with one exception (2000 $m^3 \cdot day^{-1}$ wastewater). Only 2.2% of the human population uses domestic septic tanks.

```
┌─────────────────────────┐
│  Phosphate in water sample │
│    or extract solution     │
└─────────────────────────┘
            │         Filter with a 0.45 μm membrane filter paper
┌─────────────────────────┐
│      Concentration by      │      Add MgCl₂
│  magnesium-induced co-     │      Adjust pH ~10.5 using 5 M NaOH
│   precipitation method     │
│         (MAGIC)            │
└─────────────────────────┘
            │         Dissolve the precipitation by 10 M HNO₃
            │         Filter with a glass filter paper
┌─────────────────────────┐
│   Organic mater removal²   │      Pass into column resin
└─────────────────────────┘      (Oasis HLB or Inertsep PLS-3)
            │
            │                    Adjust pH from 5.5 to 5.8 using concentrated
┌─────────────────────────┐      CH₃COOH, 10 M HNO₃, 8 M KOH
│   Precipitation as CePO₄   │      Add CeNO₃
└─────────────────────────┘
            │         Collect the precipitation by filtration
            │         Wash precipitation using 0.5 M CH₃COOK
            │         Dissolve using 1 M HNO₃
┌─────────────────────────┐
│      Cation removal        │      Add cation exchange resin (AG50x8)
└─────────────────────────┘
            │         Remove the resin by filtration
            │                    Add AgNO₃
┌─────────────────────────┐      Adjust pH to neutral using 2 M NH₄NO₃,
│    Ag₃PO₄ precipitation    │      3 M HNO₃ and concentrated NH₄OH
└─────────────────────────┘
            │
┌─────────────────────────┐
│   Organic mater removal    │      Add 15% H₂O₂
└─────────────────────────┘
            │         Collect the precipitation by filtration
            │         Wash with UPW
            │         Day at 50°C
┌─────────────────────────┐
│       IRMS analysis        │
└─────────────────────────┘
```

- **Phosphate in water sample or extract solution**
  - Filter with a 0.45 μm membrane filter paper
- **Concentration by magnesium-induced co-precipitation method (MAGIC)**
  - Add $MgCl_2$
  - Adjust pH ~10.5 using 5 M NaOH
  - Dissolve the precipitation by 10 M HNO_3
  - Filter with a glass filter paper
- **Organic mater removal[2]**
  - Pass into column resin (Oasis HLB or Inertsep PLS-3)
- **Precipitation as $CePO_4$**
  - Adjust pH from 5.5 to 5.8 using concentrated CH_3COOH, 10 M HNO_3, 8 M KOH
  - Add $CeNO_3$
  - Collect the precipitation by filtration
  - Wash precipitation using 0.5 M CH_3COOK
  - Dissolve using 1 M HNO_3
- **Cation removal**
  - Add cation exchange resin (AG50x8)
  - Remove the resin by filtration
- **Ag_3PO_4 precipitation**
  - Add $AgNO_3$
  - Adjust pH to neutral using 2 M NH_4NO_3, 3 M HNO_3 and concentrated NH_4OH
- **Organic mater removal**
  - Add 15% H_2O_2
  - Collect the precipitation by filtration
  - Wash with UPW
  - Day at 50°C
- **IRMS analysis**

Figure S1. Protocol to purify phosphate in water and source samples to obtain Ag_3PO_4 for isotope analysis. The protocol originates from McLaughlin et al.[1] with the addition of a solid-phase extraction step to remove dissolved organic matter.[2]
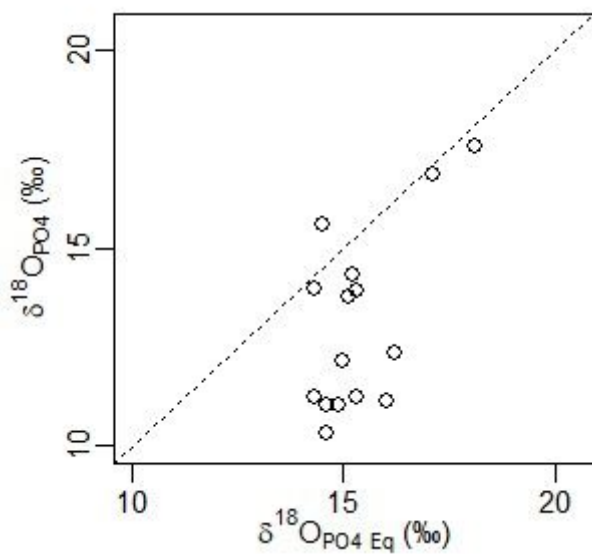
Figure S2. Relationship between $\delta^{18}O_{PO4}$ values in river water and those of isotopic exchange equilibrium with water, $\delta^{18}O_{PO4\ Eq}$. Dashed line represents $\delta^{18}O_{PO4} = \delta^{18}O_{PO4\ Eq}$.
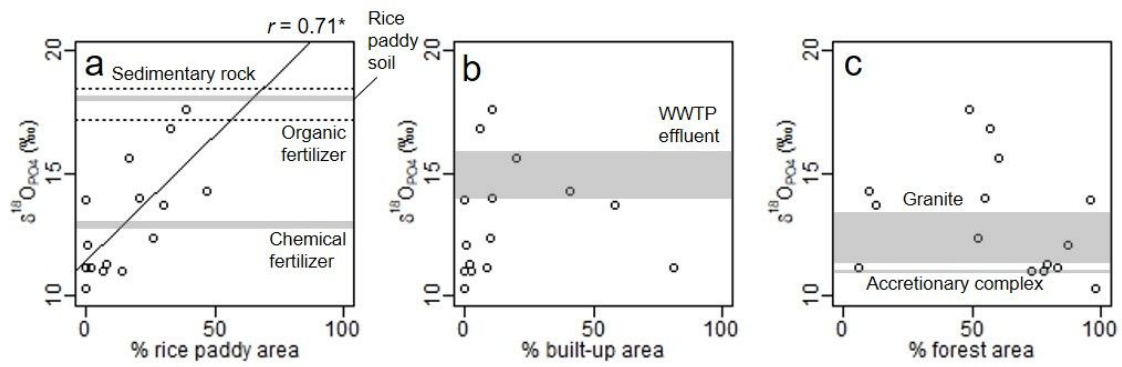
Figure S3. Correlations between river-water $\delta^{18}O_{PO4}$ and proportional area of (a) rice paddies, (b) built-up areas, and (c) forest in the catchment of the streams studied. Dotted line or shaded bars indicate the $\delta^{18}O_{PO4}$ value or range of potential P sources in each land use.

* $p < 0.05$.

Figure S4. Correlations between river-water $\delta^{18}O_{PO4}$ and proportional area of (a) bedrocks; accretionary complex, (b) granite, and (c) sedimentary rock. Dotted lines or shaded bars indicate the $\delta^{18}O_{PO4}$ value or range of HCl extraction in bedrocks.

$*\ p < 0.05$

Table S1. Hydrological characteristics and proportional area of land use and bedrock at each sampling site. IDs refer to sampling location as shown in Fig. 1.

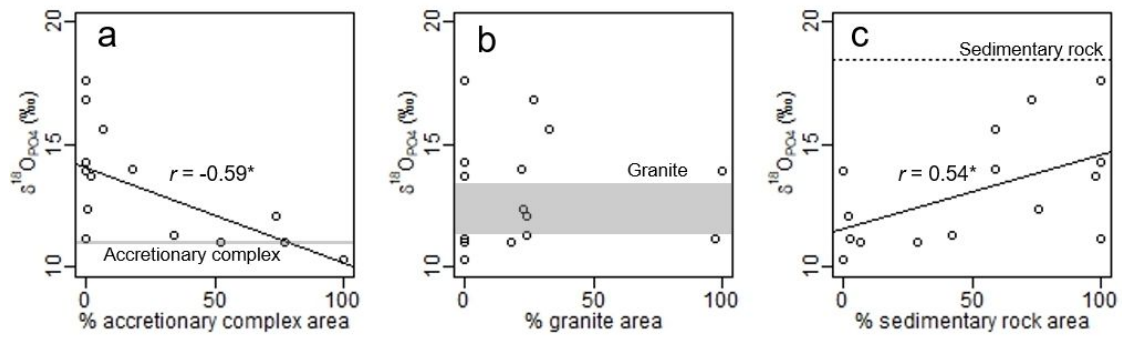| ID	Stream order	Water temperature	River width	River depth	Flow velocity	River discharge	Canopy openness	Catchment area
		°C	m	cm	cm s^{-1}	m^3 s^{-1}		km^2
3	5	23.0	29.9	35.8	37.7	3.765	0.79	387
8	1	20.2	2.68	33.1	12.5	0.102	0.54	1.72
9	2	21.0	1.64	5.04	36.6	0.030	0.35	2.18
10	2	16.5	0.82	7.04	24.9	0.013	0.25	1.01
11	1	18.4	1.80	6.04	2.38	0.002	0.39	0.99
12	2	20.2	3.54	48.5	1.59	0.024	0.66	3.60
15	3	20.7	1.64	8.28	29.5	0.037	0.47	10.3
21	4	23.4	8.16	54.3	11.7	0.483	0.65	20.7
22	3	19.8	4.98	14.3	14.2	0.093	0.38	10.7
23	1	22.1	2.10	1.28	4.12	0.001	0.66	0.25
24	2	20.1	4.08	23.2	45.2	0.417	0.31	7.04
28	2	16.2	3.62	24.2	8.62	0.070	0.60	3.24
29	3	ND	3.86	25.8	28.9	0.254	0.40	6.98
31	2	18.6	1.82	11.4	35.1	0.061	0.37	2.46
34	3	16.0	2.70	21.2	19.4	0.101	0.48	13.0
35	3	20.4	1.74	13.0	6.73	0.014	0.30	7.26
38	4	21.9	4.44	17.2	34.2	0.242	0.77	53.1
39	2	18.2	1.72	17.5	5.05	0.013	0.19	1.26
44	1	20.5	4.38	47.4	3.09	0.047	0.24	4.86
45	3	19.7	9.72	10.6	16.6	0.156	0.48	29.3
52	4	17.9	ND	ND	ND	2.870	0.70	121
54	4	16.3	25.5	32.6	39.7	3.126	0.78	70.6
55	3	17.9	15.7	22.7	27.6	0.970	0.58	48.0
56	1	14.0	1.28	6.96	6.94	0.006	0.05	0.27
57	1	16.5	1.86	12.0	8.55	0.016	0.51	0.52
61	3	17.4	11.1	25.2	43.8	1.186	0.69	25.0
62	3	13.9	3.44	19.7	14.1	0.073	0.03	1.85
64	3	15.1	16.4	54.0	22.6	1.985	0.75	39.3
70	1	12.2	4.58	23.5	17.2	0.156	0.03	0.76
201	2	13.2	10.6	14.6	77.2	1.171	0.46	6.41

ID	Proportional area of land use				Proportional are of bedrock			
	Forest	Paddy field	Built-up	Crop land	Accretionary complex	Granite	Sedimentary rock	Volcanic
	%	%	%	%	%	%	%	%
3	55	21	11	2	18	22	59	0
8	69	8	23	0	82	0	18	0
9	13	30	58	0	2	0	98	0
10	96	0	3	0	7	89	5	0
11	65	0	34	0	0	98	2	0
12	83	0	9	0	0	97	3	0
15	60	17	20	2	7	33	59	0
21	41	32	24	0	1	1	98	0
22	73	6	5	0	0	92	8	0
23	6	2	81	0	0	0	100	0
24	10	47	41	1	0	0	100	0
28	84	12	0	0	0	83	17	0
29	80	5	1	0	0	95	5	0
31	57	33	6	0	0	27	73	0
34	69	16	4	0	0	85	15	0
35	51	27	10	0	0	37	61	0
38	48	29	11	2	0	20	79	0
39	35	25	36	1	0	0	97	0
44	49	39	11	1	0	0	100	0
45	52	26	10	3	1	23	76	0
52	78	7	3	1	52	18	29	1
54	81	5	2	1	71	14	13	1
55	75	9	3	2	24	24	51	1
56	96	0	0	0	0	100	0	0
57	73	14	0	13	77	0	7	17
61	79	8	2	1	34	24	42	0
62	95	5	0	0	85	0	11	4
64	87	1	1	0	74	24	2	0
70	98	0	0	0	100	0	0	0
201	92	0	2	0	62	34	1	3

Table S2. SRP concentrations and fluxes, measured $\delta^{18}O_{PO4}$ values, oxygen isotope values of water, water temperature and equilibrium $\delta^{18}O_{PO4}$ values of Yasu river water. IDs refer to sampling location as shown in Fig. 1. ND means not detected. NA means not available.

ID	Sample type	SRP		$\delta^{18}O_{PO4}$	$\delta^{18}O_{H2O}$	Water temp.	$\delta^{18}O_{PO4\ Eq}$
		Concentration	Flux				
		μmol L^{-1}	mmol day^{-1}	‰	‰	°C	‰
3	River water	1.35	439	14.0	-6.25	23.0	14.3
8	River water	0.65	5.66	NA	-6.95	20.2	14.3
9	River water	0.42	1.07	13.7	-5.95	21.0	15.1
10	River water	1.35	1.47	NA	-7.96	16.5	14.1
11	River water	3.81	0.63	NA	-7.53	18.4	14.1
12	River water	2.34	4.93	11.2	-6.91	20.2	14.3
15	River water	3.08	10.0	15.6	-6.57	20.7	14.5
21	River water	1.97	82.6	NA	-5.69	23.4	14.8
22	River water	1.14	9.17	NA	-7.26	19.8	14.0
23	River water	0.35	0.03	11.2	-4.76	22.1	16.0
24	River water	0.35	12.8	14.3	-6.04	20.1	15.2
28	River water	0.42	2.55	NA	-6.77	16.2	15.4
29	River water	0.35	7.78	NA	-6.61	NA	NA
31	River water	0.65	3.38	16.8	-4.44	18.6	17.1
34	River water	0.42	3.67	NA	-6.39	16.0	15.8
35	River water	0.16	0.20	NA	-4.72	20.4	16.4
38	River water	0.17	3.51	NA	-5.34	21.9	15.5
39	River water	0.87	0.99	NA	-5.97	18.2	15.7
44	River water	2.08	8.49	17.6	-3.05	20.5	18.1
45	River water	1.41	19.0	12.4	-5.12	19.7	16.2
52	River water	2.83	701	11.0	-7.11	17.9	14.6
54	River water	2.05	554	NA	-7.32	16.3	14.8
55	River water	3.32	278	NA	-6.51	17.9	15.2
56	River water	1.51	0.73	13.9	-7.30	14.0	15.3

57	River water	2.98	4.05	11.0	-7.13	16.5	14.9
61	River water	3.51	360	11.3	-6.56	17.4	15.3
62	River water	ND	0.41	NA	-6.81	13.9	15.9
64	River water	ND	11.1	12.1	-7.37	15.1	15.0
70	River water	ND	0.87	10.3	-8.46	12.2	14.6
201	River water	0.16	16.3	NA	-7.41	13.2	15.4

Table S3. SRP concentration and flux, measured $\delta^{18}O_{PO4}$, oxygen isotope values of water, water temperature and equilibrium $\delta^{18}O_{PO4}$ values of WWTP effluent. IDs refer to sampling location as shown in Fig. 1.

ID	Sample type	SRP		$\delta^{18}O_{PO4}$	$\delta^{18}O_{H2O}$	Water temperature	$\delta^{18}O_{PO4\ Eq}$
		Concentration	Flux				
		$\mu mol\ L^{-1}$	mmol day^{-1}	‰	‰	°C	‰
W1	WWTP effluent	5.20	22.1	14.0	-7.47	26.0	12.4
W2	WWTP effluent	48.0	20.4	15.9	-7.08	26.9	12.6
W3	WWTP effluent	39.3	8.85	15.6	-7.34	24.6	12.8
W4	WWTP effluent	81.9	23.1	15.1	-6.98	29.1	12.1
W5	WWTP effluent	56.1	21.5	15.1	-7.58	27.7	11.9
W6	WWTP effluent	116	63.6	15.9	-7.48	27.3	12.1

Table S4. P concentrations and measured $\delta^{18}O_{PO4}$ values of solid P sources: bedrocks (R), soils (S), and fertilizers (F). IDs refer to sampling location as shown in Fig. 1. ND means no data.

ID	Sample type	Extract solution	P concentration	$\delta^{18}O_{PO4}$
			mmol kg^{-1}	‰
R1	Accretionary complex	1 M HCl	10.2	11.1
R2	Accretionary complex	1 M HCl	3.14	11.0
R3	Granite	1 M HCl	2.34	11.4
R4	Granite	1 M HCl	0.21	13.4
R5	Sedimentary rock	1 M HCl	4.41	18.5
S1	Rice paddy soil	0.5 M NaHCO$_3$	3.58	18.2
S2	Rice paddy soil	0.5 M NaHCO$_3$	2.89	18.0
S3	Forest soil	0.5 M NaHCO$_3$	0.07	ND
S4	Forest soil	0.5 M NaHCO$_3$	0.04	ND
S5	Forest soil	0.5 M NaHCO$_3$	0.05	ND
S6	Forest soil	0.5 M NaHCO$_3$	0.06	ND
S7	Forest soil	0.5 M NaHCO$_3$	0.06	ND
S8	Forest soil	0.5 M NaHCO$_3$	0.07	ND
S9	Forest soil	0.5 M NaHCO$_3$	0.05	ND
S10	Forest soil	0.5 M NaHCO$_3$	0.02	ND
F1	Organic fertilizer	Water	48.6	17.2
F2	Chemical fertilizer	Water	254	12.7
F3	Stock solution	None	ND	13.1

Table S5. Pearson correlation coefficients between proportional area of each land use and lithological type at 15 sites where $\delta^{18}O_{PO4}$ values of river water were obtained

* $p < 0.05$

Variable	Forest	Rice paddy	Built-up	Accretionary complex	Granite	Sedimentary rock
Forest		-	-	-	-	-
Rice paddy	-0.62*		-	-	-	-
Built-up	-0.88*	0.22		-	-	-
Accretionary complex	0.57*	-0.46	-0.46		-	-
Granite	0.51	-0.44	-0.36	-0.30		-
Sedimentary rock	-0.91*	0.76*	0.70*	-0.65*	-0.52*	

REFERENCES

(1)   McLaughlin, K.; Silva, S.; Kendall, C.; Stuart-Williams, H.; Paytan, A. A Precise

Method for the Analysis of $\delta^{18}O$ of Dissolved Inorganic Phosphate in Seawater.

Limnol. Oceanogr. Methods **2004**, *2*, 202–212.

(2)   Mellett, T.; Selvin, C.; Defforey, D.; Roberts, K.; Lecher, A. L.; Dennis, K.;

Gutknecht, J.; Field, C.; Paytan, A. Assessing Cumulative Effects of Climate

Change Manipulations on Phosphorus Limitation in a Californian Grassland.

Environ. Sci. Technol. **2018**, *52* (1), 98–106.